Acta Oceanol. Sin., 2019, Vol. 38, No. 8, P. 78–85
https://doi.org/10.1007/s13131-019-1389-3
http://www.hyxb.org.cn
E-mail: hyxbe@263.net

Fast acclimation of phytoplankton assemblies to acute salinity stress in the Jiulong River Estuary

Gang Li[1]*

[1] Key Laboratory of Tropical Marine Bio-resources and Ecology & Guangdong Provincial Key Laboratory of Applied Marine Biology, South China Sea Institute of Oceanology, Chinese Academy of Sciences, Guangzhou 510301, China

Received 18 May 2018; accepted 3 July 2018

Abstract

Mixing of freshwater and seawater creates the well-known salinity gradients along the estuaries. In order to investigate how phytoplankton respond to the acute salinity changes, we exposed natural phytoplankton assemblies from the Jiulong River Estuary to differential saline field water while continuously monitoring their photosynthetic performances under both indoor- and outdoor-growth conditions. When the natural cell assemblies from salinity 30 field water were exposed to series low saline field water (salinity 25, 17, 13 and 7.5), the effective Photosystem II quantum yield ($\Delta F/F_m'$) decreased sharply, e.g., to one-fifth of its initials after 5 min exposure to salinity 7.5 field water, and then increased fast during the following 40 min and almost completely recovered after 320 min. During such an exposure process, non-photochemical quenching (NPQ) sharply increased from 0 to 0.85 within 5 min, and then decreased to nearly 0 within the following 70 min. When these cells re-acclimated to salinity 7.5 field water were exposed to series high saline field water (salinity 13, 17, 25 and 30), a similar response pattern was observed, with the decreased $\Delta F/F_m'$ accompanied with increased NPQ, and followed by the recovery-induced increase in $\Delta F/F_m'$ and decrease in NPQ. A similar response pattern as $\Delta F/F_m'$ to the acute osmotic stress was also observed in the photosynthetic carbon fixation capacity according to radiocarbon (^{14}C) incorporation. Our results indicate that estuarine phytoplankton assemblies could rapidly recover from the acute osmotic stress, implying a potential cause for their frequent blooms in coastal-estuarine waters where despite drastically varying salinity, available nutrients are abundant due to the land-derived runoffs or mixing-caused relaxations from sediments.

Key words: PSII quantum yield, carbon fixation, salinity gradients, phytoplankton assemblies, Jiulong River Estuary

Citation: Li Gang. 2019. Fast acclimation of phytoplankton assemblies to acute salinity stress in the Jiulong River Estuary. Acta Oceanologica Sinica, 38(8): 78–85, doi: 10.1007/s13131-019-1389-3

1 Introduction

In estuaries, mixing of freshwater and seawater often creates the well-known salinity gradients, from pure freshwater near the head of the estuary to seawater near the mouth of the estuary. This salinity gradient exerts a non-negligible impact on the physiology of phytoplankton, such as decreasing photosynthesis and increasing respiration, and subsequently reducing growth (Rijstenbil et al., 1989a, b ; Lu and Zhang, 1999; D'ors et al., 2016), and even altering species communities (Licursi et al., 2006; Li et al., 2014; Wang et al., 2015b). Thus, the continuous salinity gradients in estuaries are often considered as one of the main drivers to shift the distributions of phytoplankton biomass and species compositions (Licursi et al., 2006; Muylaert et al., 2009). Usually, freshwater species of phytoplankton are replaced by marine ones when the salinity varies from 0.5 to 10 in estuaries (Huang et al., 2004; Domingues et al., 2010; Li et al., 2011a, 2014). According to the reports of Li et al. (2011b), succession of dominant species occurred from typical freshwater chlorophytes (e.g., *Scenedesmus* spp.) below salinity 5 to marine diatoms (e.g., *Skeletonema costatum*, *Chaetoceros* sp. and *Coscinodiscus* spp.) above salinity 10 in the Jiulong River Estuary. Similarly, the green algae and cryptophytes were also observed as dominant species in lower saline water in South African estuaries, dinoflagellates in marine-brackish water, whereas diatoms and cyanobacteria dominated in hypersaline conditions (Nche-Fambo et al., 2015). Such a species succession along the salinity gradient is often attributed to the fact that these phytoplankton species are stenohaline and suffer from the osmotic stress when they are exposed to changing salinity (Licursi et al., 2006; D'ors et al., 2016). In cyanobacteria *Spirulina platensis*, the salt stress has been detected to cause the decrease in Photosystem II (PSII) activity and increase in PSII susceptibility to photoinhibition (Lu and Zhang, 1999); while in diatoms, e.g., *Skeletonema costatum* and *Ditylum brightwellii*, this salt stress has been observed to induce the increase in cellular small amino acids pools and in turn to enhance cellular osmolity (Rijstenbil et al., 1989a, b). Bloom of phytoplankton has

Foundation item: The National Natural Science Foundation of China under contract Nos 41890853 and 41676156; the National Basic Research Program of China (973 Program) under contract No. 2015CB452903; the Strategic Priority Research Program of Chinese Academy of Sciences under contract Nos XDA13020103 and XDA11020305; the Natural Science Foundation of Guangdong Province under contract Nos 2015A030313826 and 2017A030313216; the Special Fund for Agro-scientific Research in the Public Interest under contract No. 201403008; the Science and Technology Planning Project of Guangdong Province under contract No. 2017B030314052.
*Corresponding author, E-mail: ligang@scsio.ac.cn

been reported to associate regularly with low salinity of the estuarine areas or coastal regions (Lim and Ogata, 2005). Such as the blooms of dinoflagelate *Alexandrium minutum* coincided with increasing rainfalls and freshwater runoffs in the Mediterranean Sea (Giacobbe et al., 1996). Similar findings were also reported about the blooms of diatom *Pseudo-Nitzschia multiserie* under lower salinity conditions (Doucette et al., 2008) and abundant diatoms *Pseudo-Nitzschia* spp. in coastal areas where salinity varied widely (Thessen et al., 2005). In estuaries, the tide-induced intrusion of open sea water usually extends to far upstream (Wang et al., 1986), which leads to an intensely turbulent diffusion at estuarine axis (Liu et al., 2008) and mixes the seawater-thrived phytoplankton up to freshwater (Li et al., 2011b). However, little has been documented about how these phytoplankton groups respond to such an acute salinity change, despite it is of great importance in understanding the causes for frequent phytoplankton blooms and species dynamics in estuaries.

The Jiulong River Estuary (Fig. 1) is strongly influenced by tidal changes. Therefore, drastic salinity changes prevail this estuary, with the salinity-decrease rate reached as high as 6.7 km^{-1} at interface between seawater and freshwater (Liu et al., 2008). Additionally, rapid economic development along this estuary has accelerated its eutrophication process during the last decades (Yan et al., 2012; Wu et al., 2017), leading to the frequent occurrence of algal blooms (Cao et al., 2005; Tang et al., 2010; Chen et al., 2012); thus, more and more attentions have recently been paid to the ecological status of this estuary, including to characterize its hydrodynamics (Liu et al., 2008; Wang et al., 2013), investigate its chemical environments (Yan et al., 2012; Chen et al., 2013a, b; Cao et al., 2015; Wang et al., 2015a), depict its biological features (Liu et al., 2013; Zhang et al., 2013; Tian et al., 2014) and analyze the relationships between biotic and abiotic properties (Li et al., 2011a; Chen et al., 2012; Wang et al., 2015b). However, studies focused on the physiology of phytoplankton are scarce (Li et al., 2011b), which limits our full understanding of this estuarine ecosystem. In this paper, we therefore aimed to experimentally test the physiological responses of phytoplankton to the acute field salt stress and to particularly examine their acclimation processes in the Jiulong River Estuary. Experiments with natural phytoplankton assemblies were conducted to test the effects of acute salt stress on the photosynthetic effective quantum yield and carbon fixation.

2 Materials and methods

2.1 *Sampling area and protocols*

The Jiulong River Estuary (Fig. 1) has a watershed area of about 130 km^2 and water depth of 3–16 m. Less than 25% amount of freshwater inflow occurs in dry season from October to next March when surface maximum tidal current speeds can be over

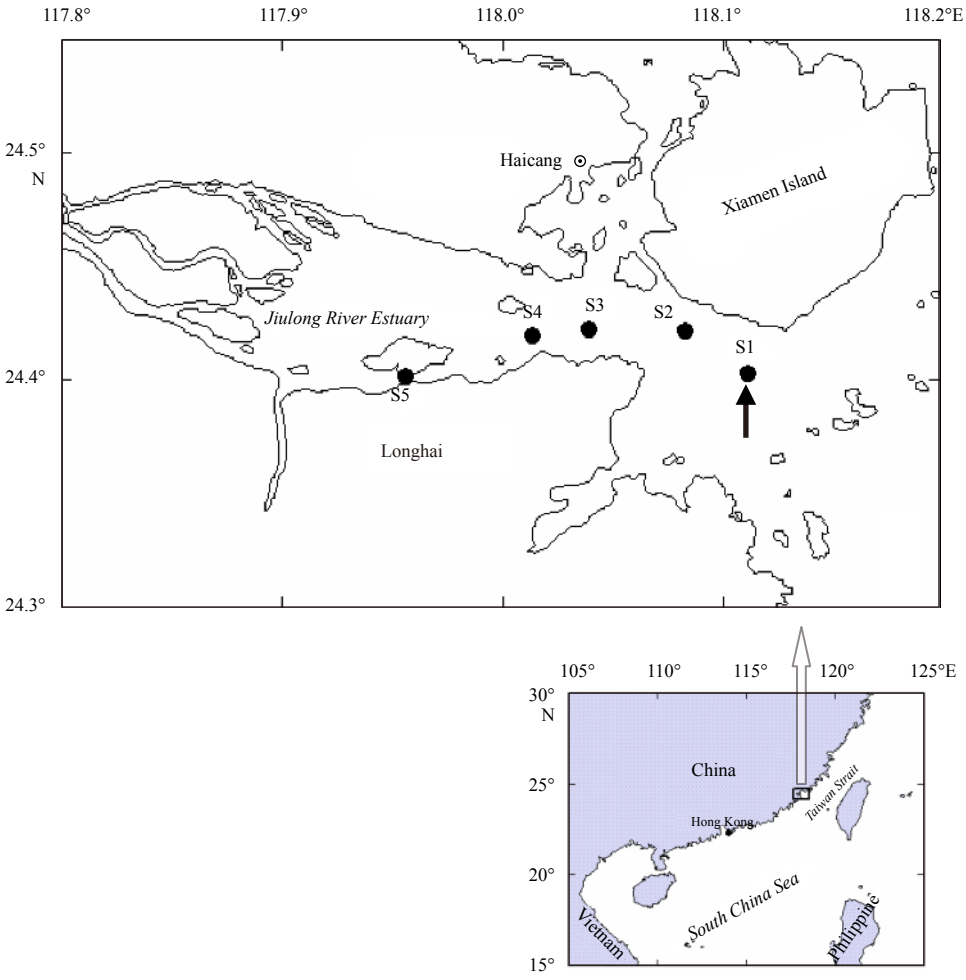

Fig. 1. Map of the Jiulong River Estuary (upper panel) and its location in the coasts of China's seas (lower panel) showing the sites where phytoplankton assemblies were collected (S1 marked with arrow) and where the field water was collected (S1–S5).

2.5 m/s in spring tide, leading to more drastic salinity gradient (Cai et al., 1991). Therefore, we carried out the experiments in dry season (November 2007 and February 2008) to determine the physiological responses of phytoplankton assemblies to the acute salinity changes in this estuary.

Surface seawater was collected using 15 L acid-clean (1 mol/L HCl) carboys at five stations with five salinity levels [S1, S2, S3, S4 and S5; 30, 25, 17, 13 and 7.5] along this estuary (Fig. 1). After returning to laboratory within 2 h, part of the collected water was vacuum-filtrated through Whatman GF/F glass fiber filters (47 mm in diameter) and stored at 4°C for later use. Simultaneously, phytoplankton assemblies from S1 (salinity 30) were collected using a 20 μm-pore Nitex® mesh, gently removed into the f/2-enriched filtrated salinity 30 field water, and cultivated for 5 d in an incubator (200 μmol photons m^{-2} s^{-1}; 25°C; 12:12 light:dark) with 0.5 L/min aeration. The assemblies were termed as the high-saline cell assemblies, which were then inoculated to the f/2-enriched salinity 7.5 field water (S5) and cultivated for another three weeks to obtain the low-saline cell assemblies. Both the high- (salinity 30) and low-saline (salinity 7.5) cell assemblies were used for the following experiments. In addition, the collected water samples were pre-filtrated over a 180 μm-pore mesh before collecting phytoplankton cell assemblies, to eliminate as much effects of zooplankton as possible. During sampling period, the phytoplankton assemblies with the effective diameter of >20 μm took up approximately 40% of total chlorophyll *a* (Chl *a*) concentration.

2.2 *Experiment design*

Experiment I: In an incubator mentioned above, 2 mL culture with high- or low-saline-grown cell assemblies (salinity 30 or 7.5) was inoculated into duplicate 50 mL filtrated field water of salinity 7.5, 13, 17, 25 and 30 (see above), making Chl *a* as similar as *in situ* status. After transferring high-saline cell assemblies to series low saline field water, Chl *a* fluorescence was monitored at time-points of 5, 20, 40, 70, 120, 180, 240 and 320 min using an Xe-PAM (Waltz, Effeltrich, Germany). Similarly, Chl *a* fluorescence of low-saline cell assemblies (salinity 7.5) that were transferred to series high saline water was continuously monitored within 250 s and the following time-points of 2, 20, 50, 120 and 200 min. The effective photosystem II (PSII) quantum yield ($\Delta F/F_m'$) and non-photochemical quenching (NPQ) under 200 μmol photons m^{-2} s^{-1} growth light were calculated according to Genty et al. (1989) and Van Kooten and Snel (1990), with saturating pulse of 4 800 μmol photons m^{-2} s^{-1} for 600 ms.

(1) $\Delta F/F_m' = (F_m'-F_t)/F_m'$, where F_m' is the maximum fluorescence under growth light, and F_t is the steady state fluorescence of light-adapted cells;

(2) $NPQ = (F_m-F_m')/F_m'$, where F_m is the maximum fluorescence yield after 5 min dark adaptation, and F_m' is the maximum fluorescence under growth light. Here we used the F_m values of time 0 of the control for NPQ calculation.

Experiment II: 5 mL of high-saline (salinity 30) cell assemblies were inoculated into duplicate 150 mL quartz tubes filled with series pre-filtrated field low-saline water (salinity 7.5, 13, 17, 25 and 30) with Chl *a* similar to *in situ* level, incubated in a water tank and exposed to solar radiation (UVR was removed by 395 filter (Li et al., 2011b) to roughly equal the light quality in incubator or to simplify the comparisons). We did two sets of outdoor incubated experiments that lasted from 7:00 am to 18:00 pm on November 11 and 12, 2008. During the incubations we took 5 mL sample from each treatment every hour and measured the effective PSII yield ($\Delta F/F_m'$) with the Xe-PAM.

Experiment III: Under a metal halide lamp (200 μmol photons m^{-2} s^{-1}), 10 mL of high-saline (salinity 28) cell assemblies (salinity at Site S1 was 28 on February 28 of 2009) was inoculated to triplicate flasks that were filled with 240 mL pre-filtrated field water (salinity 28, 20, 15 and 7 at S1, S3, S4 and S5), making Chl *a* content similar to the *in situ* status. The flasks were incubated in a water tank for temperature control (25°C). At time-points of zero (0), 60 min and 180 min, 80 mL sample from each flask was dispensed into a tube, and spiked with 50 μL–2.5 μCi (92.5 kBq) $Na^{14}HCO_3$ solution (ICN Radiochemicals, USA) and incubated back to the water tank for additional 40 min. After the incubation, the sample was filtrated onto a Whatman GF/F glass fiber filter (25 mm in diameter); and the filters with samples were placed into a 20 mL scintillation vial and exposed to HCl fumes overnight and dried (55°C, 6 h) to remove the unfixed ^{14}C. Then, 3 mL scintillation cocktail (UltimaGold, Perkin Elmer®) was added to each vial and the incorporated ^{14}C was measured with a liquid scintillation counter (Tri-carb 2800TR, Perkin Elmer, USA). Photosynthetic carbon fixation rate was calculated according to Holm-Hansen and Helbling (1995).

2.3 *Environment determinations*

Salinity and temperature in sampling sites were measured with a SONDE (YSI 600QS, Yellow Spring Instruments, USA). Light intensity in incubator was measured with a lux meter (TES 1332A, Taiwan). Outdoor incident solar radiation was monitored with a broadband filter radiometer (ELDONET, Real Time Computers, Inc., Germany) that was settled on the roof of Ocean Building of Xiamen University; this equipment measures the solar irradiation every second in UV-B (280–315 nm), UV-A (315–400 nm) and PAR (400–700 nm) wavebands and records the minute-averaged values. The units of light are unified by 1 W/m^2 = 5.0 μmol photons m^{-2} s^{-1} = 26.5 lx.

To measure dissolved inorganic nitrogen, phosphate and silicate contents, 800 mL surface water was collected at each station, and stored at 4°C until the analyses were performed within 6 h in laboratory. Nitrate, nitrite and ammonium were determined colorimetrically according to Wood et al. (1967) and Pai et al. (2001), and phosphate and silicate were manually determined according to Murphy and Riley (1962) and Armstrong et al. (1967).

2.4 *Chl a measurement and species analysis*

To measure Chl *a* content, aliquots of samples (300–500 mL for field water or 100 mL for culture) were filtrated onto a Whatman GF/F filter (25 mm in diameter), extracted in 5 mL absolute methanol in the dark for 3 h at room temperature of 23–25°C. After centrifugation, the optical density of the extract was measured with a scanning spectrophotometer (DU800, Beckman Counter, USA). Chl *a* concentration was calculated using the equation of (Porra, 2002).

For species analysis, the field water samples or cultures were fixed with buffered formalin (final concentration of 0.4%). According to Villafañe and Reid (1995), the samples were settled in a 50 or 10 mL cylinder of an Utermöhl Chamber (Hydro-Bios Kiel, Germany) for 24 h, qualitative and quantitative analyses were carried out under an inverted microscope (IX51, OLYMPUS, Japan).

2.5 *Statistical analysis*

Data are shown as mean and errors (i.e., standard deviations for three replicates and half of range for two replicates) in figures. Statistical analysis was performed using Paired *t*-test or one-way

ANOVA with significant level at $p<0.05$.

3 Results

From the open sea water going upstream to the tidal limit water of the Jiulong River Estuary, salinity decreased by 1.24 km^{-1} from 30.4 (S1) to 7.52 (S5) and the euphotic zone depth decreased from 3.68 to 0.18 m (Table 1). The concentrations of dissolved inorganic nitrogen (DIN) increased from 38.6 to 145 μmol/L and silicate increased (SiO_3^{2-}) from 58.2 to 241 μmol/L; while that of phosphate (PO_4^{3-}, 2.74–3.48 μmol/L) showed a limited change (Table 1). Field Chl *a* content increased from 1.92 to 6.01 μg/L during the sampling period (Table 1).

Table 1. Physicochemical and biological factors of the sampling sites: salinity (S), temperature (T, °C), dissolved oxygen (DO, mg/L), concentrations (μmol/L) of dissolved inorganic nitrogen (DIN), phosphate (PO_4^{3-}) and silicate (SiO_3^{2-}), euphotic zone depth (Z_{EU}, m) and chlorophyll *a* biomass (Chl *a*, μg/L)

Stations	S	T	DO	DIN	PO_4^{3-}	SiO_3^{2-}	Z_{EU}	Chl *a*
S1	30.4	25.6	5.84	38.6	2.74	58.2	3.68	1.92
S2	25.0	25.6	6.54	62.9	3.39	96.4	3.13	1.98
S3	17.3	25.7	6.42	115	3.48	186	1.07	1.56
S4	13.3	25.8	5.75	123	3.42	196	0.77	2.97
S5	7.52	25.7	5.16	145	3.45	241	0.18	6.01

Photosynthetic performances of the high-saline (salinity 30) cell assemblies changed greatly when being transferred to low-saline field water, with different extent depending on the degree that salinity changed (Fig. 2). For example, effective PSII quantum yield ($\Delta F/F_m'$) sharply decreased from 0.67 to 0.14 within 5 min when being transferred to salinity 7.5 water (S5), followed by a marked increase to 0.45 in the following 40 min and then a gradual increase to 0.61 within 320 min, to the similar as control (Fig. 2a). Oppositely, non-photochemical quenching (NPQ) showed a sudden increase from 0 to 0.85 when being transferred to salinity 7.5 water, and decreased nearly to 0 within 70 min and stayed steady till the end of the experiments (Fig. 2b). When the high-saline cell assemblies were transferred to series intermediate salinity field water (salinity 13, 17 and 25), similar response pattern was observed, that is, decreased $\Delta F/F_m'$ at first, then recovery leading to increased $\Delta F/F_m'$ and decreased NPQ (Fig. 2). A similar response pattern also occurred when transferred low-saline (salinity 7.5) cell assemblies to series high-saline field waters (salinity 13, 17, 25 and 30), i.e., the quantum yield sharply decreased at first 2 min, then gradually increased and almost completely recovered within the following 200 min (Fig. 3a); while NPQ markedly increased at first then decreased to nearly 0 in the following 50 min and kept steady till the end of the experiments (Fig. 3b). The durations of the decrease of $\Delta F/F_m'$ lasted 20 s after the acute salinity changes of 7.5 to 30 (Fig. 3a inset).

In outdoor conditions, phytoplankton assemblies showed

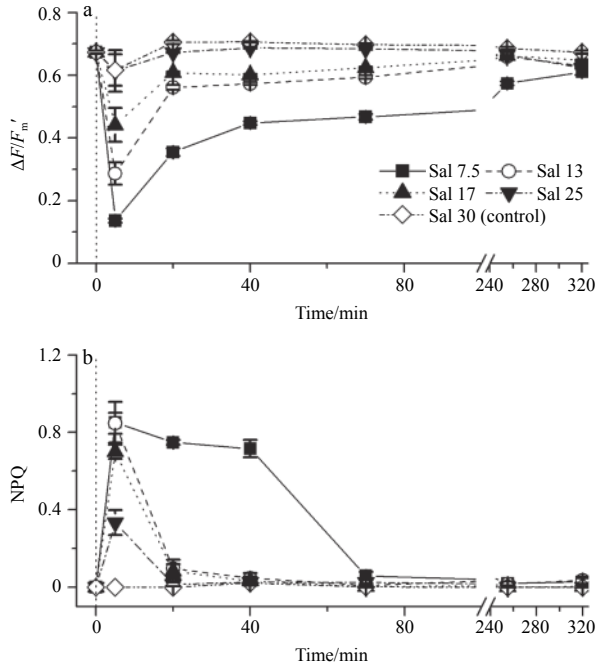

Fig. 2. Time-series variations of effective PS II quantum yield (a, $\Delta F/F_m'$) and non-photochemical quenching (b, NPQ) by exposing the high-saline (salinity 30) cell assemblies to salinity 7.5, 13, 17, 25 and 30 field water. Vertical bars represent standard deviations (n=6). Sal represents salinity.

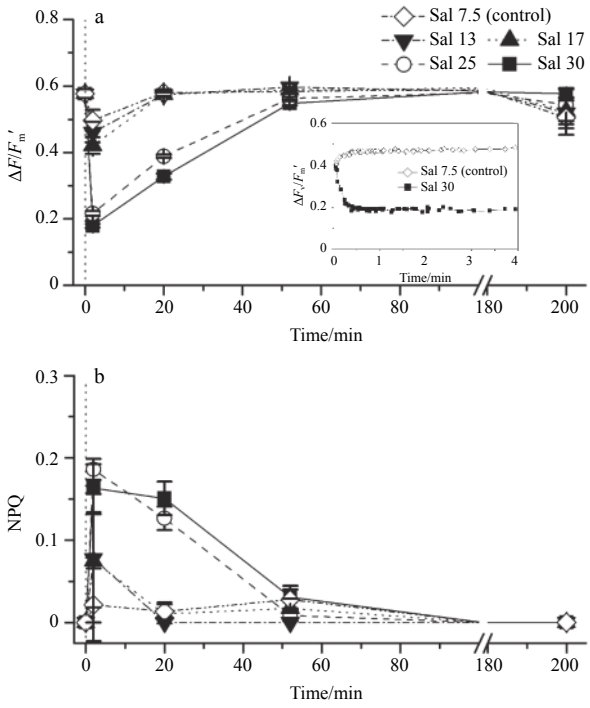

Fig. 3. Time-series variations of effective PS II quantum yield (a, $\Delta F/F_m'$) and non-photochemical quenching (b, NPQ) by exposing low-saline (salinity 7.5) cell assemblies to salinity 7.5, 13, 17, 25 and 30 field water. The insert figures showed a representative variation of $\Delta F/F_m'$ by exposing the salinity 7.5 cell assemblies to salinity 30 field water during the first 4 min. Vertical bars represent standard deviations (n=6).

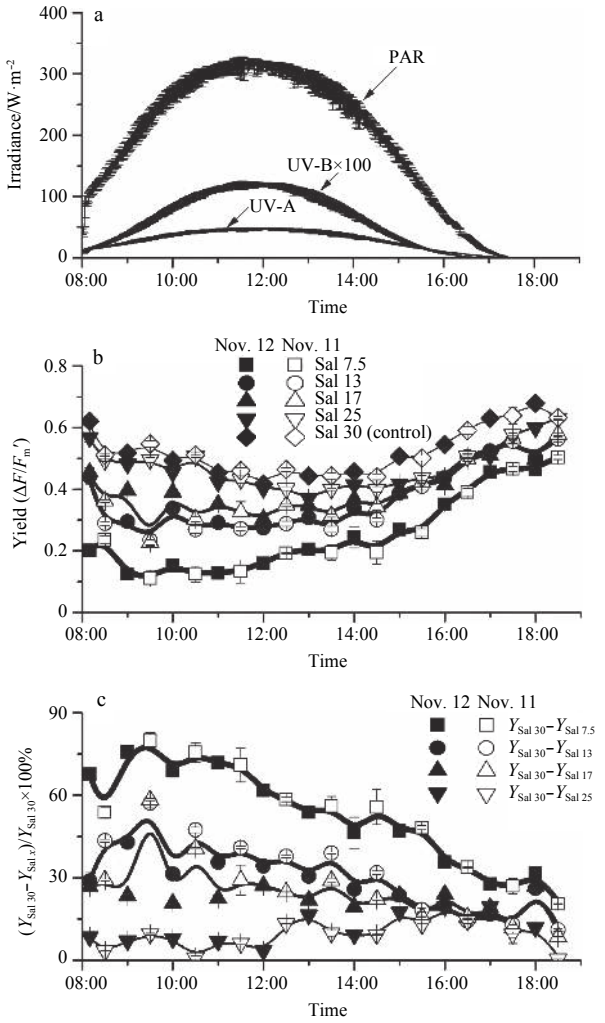

Fig. 4. Mean incident solar irradiance (a) of PAR (400–700 nm), UV-A (315–400 nm) and UV-B (280–315 nm) in W/m², on November 11 and 12, 2008; daily variations of effective PS II quantum yield ($\Delta F/F_m'$) (b) and environmental stress (%) (c) under solar PAR by exposing high-saline (salinity 30) cell assemblies to salinity 7.5, 13, 17, 25 and 30 field water. Vertical bars represent half of ranges in a (n=2) and standard deviations in b (n=6).

similar photochemical performances as that in indoor conditions (Fig. 4). As solar PAR irradiation increased from dawn to noon (Fig. 4a), the $\Delta F/F_m'$ of high-saline (salinity 30) cell assemblies decreased (Fig. 4b), and it then gradually increased up to initials in dusk. When the high-saline cell assemblies were exposed to lower-saline field water, the $\Delta F/F_m'$ displayed a sudden decrease in morning, followed by a gradual increase to noon and finally up to the similar values as control in dusk (Fig. 4b). Consistently, the environmental stress, defined as: $(Y_{Sal\ 30} - Y_{Sal\ x})/Y_{Sal\ 30} \times 100\%$, displayed an opposite trend as $\Delta F/F_m'$ and decreased throughout the day (Fig. 4c), for e.g. the stress degree decreased from 80% to 21% from dawn to dusk when the high-saline (salinity 30) cell assemblies were transferred to low-saline (salinity 7.5) field water. Particularly, the lowest values of $\Delta F/F_m'$ in most salinity treatments occurred before 10:00 am but not 12:00 am when solar irradiation was highest (Fig. 4b), indicating the interactive light shock effects from dawn to noon upon the photosynthetic capacity.

Photosynthetic carbon fixation rate of high-saline cell assemblies reached 2.54 μg C (μg Chl a)$^{-1}$ h^{-1} in salinity 28 field water; it sharply decreased by 41% after 20 min exposure to salinity 7.5 field water, and by 8.9% and 5.9% to intermediate salinity 15 and salinity 20 field water, respectively (Fig. 5). However, the carbon fixation rate under the salt stressful condition (i.e., high-saline cell assemblies were exposed to low-saline field water) markedly increased with increasing incubated duration, and showed even no significant differences (p>0.05) among the control (salinity 28), salinity 15 and salinity 20 treatment conditions after 200 min (Fig. 5).

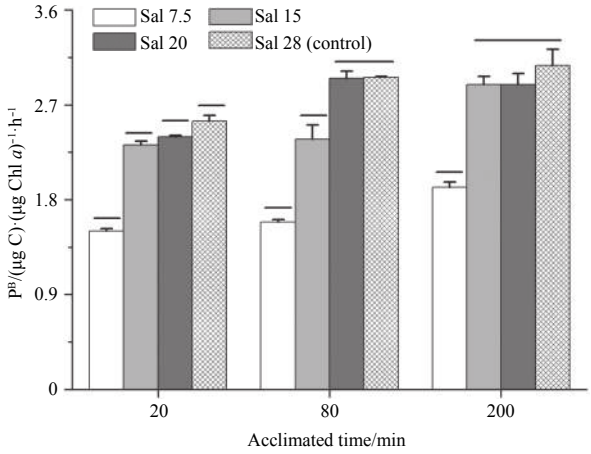

Fig. 5. Time-series variations of photosynthetic carbon fixation rate (P^B, μg C (μg Chl a)$^{-1}$ h^{-1}) after exposing high-saline (salinity 28) cell assemblies to salinity 7, 15, 20 and 28 field water. Vertical bar represents one standard deviation (n=3), whereas horizontal line represents the significant differences among salinity treatments (p<0.05).

4 Discussion

Freshwater runoffs and tidal-induced exchanges with open sea water often drastically change the salinity along the estuaries, osmotically stressing phytoplankton therein. In the Jiulong River Estuary however, phytoplankton species are often plentiful (Li et al., 2011b; Huang et al., 2012) and even bloom (Li et al., 2011a). Such a contradiction of salt stress and abundant phytoplankton in this estuary spikes our interest to study the physiological responses of phytoplankton to the acute salinity changes. We found that the seawater-thrived phytoplankton assemblies from this estuary could recover within several hours from the field osmotic stresses on the base of chlorophyll fluorescence and carbon fixation, implying their fast acclimations to the acute salinity changes and subsequent blooms.

Apart from light limitation (Cloern, 1999), the salinity changes are usually over the burden of phytoplankton cells in estuaries, thus causing the great increase in respiration and decrease in photosynthesis and growth (Rijstenbil et al., 1989a, b; Lu and Zhang, 1999; D'ors et al., 2016), and even making the cells to die (Licursi et al., 2006). In this view of the point, estuarine environments are rough and not suitable for phytoplankton to grow well (Cloern, 1999) although the nutrients contents therein e.g. nitrogen (N) and phosphorus (P) are usually high due to the land-derived runoffs and mixing-caused relaxations from sediments (Li et al., 2011b, 2014; Yan et al., 2012). On the other hand, the excessive N loads often create a surplus supply of estuarine N,

leading P to be relatively scarce and again negatively limiting the growth of phytoplankton, e.g., in the Jiulong River Estuary (Mo et al., 2013) or Pearl (Zhujiang) River Estuary (Yin et al., 2001; Yi et al., 2014). Moreover, osmotic stress induced by salinity changes has been shown to suppress the synthesis of e.g. D1 protein at both the transcriptional and translational levels (Allakhverdiev et al., 2002), which may again cause the decrease in photosynthetic activity of photosystem II (Figs 2–4) and carbon fixation (Fig. 5). In many estuaries however, high nutrients contents usually favor the growth of phytoplankton, which could overrun the adverse effects of salt stress or light limitation and make them to grow well and even bloom (Huang et al., 2004; Li et al., 2011a, 2014; Gao et al., 2018). According to Brand (1984), most phytoplankton species from the estuaries are more euryhaline than those from coastal or oceanic waters, which may make them to better tolerate the osmotic stress and thus lead them to be more abundant. What's more, it is common that primary inhibition of photosynthetic activity by salt stress is followed by partial or full restoration, but the time required for recovery is species-specific and depends on the osmotic stress degree (Radchenko and Il'iash, 2006). For example, the osmotic stress was testified to stimulate the production of intracellular ROS, but it does not induce cellular toxicity before ROS formation exceeding antioxidant defense capability or disrupting redox signaling, and affecting cell functionality (Häubner et al., 2014). Our results showed that phytoplankton assemblies from the Jiulong River Estuary could rapidly (i.e., within several hours) recover from the acute osmotic stresses, under either indoor (Figs 2 and 3) or outdoor conditions (Fig. 4), which not only contributes to the explanations about the better adaptation of estuarine phytoplankton to the acute salinity changes but also implies a potential reason why phytoplankton often bloom in this estuary although the environments therein are rough for their growing if considering the drastic salinity changes.

Differential nutrients levels among the five sampling sites (Table 1) might temper our findings, although the acute osmotic stress was not covered by the nutrient changes (Figs 2–4). Moreover, the dominant species are *Nitzschia longissima* and *Thalassiosira* spp. after the 5-day-indoor cultivation of natural cell assemblies in f/2-enriched field water, and no significant difference was observed between indoor and outdoor species compositions (data not shown). It indicates the elimination of the effects of environmental changes from outdoor- to indoor- condition, as well as the elimination of the effects of zooplankton prey by pre-filtrating the sample through a 180 μm-pore mesh before collecting phytoplankton assemblies. Thus, our cell assemblies could still mimic the field condition, despite we indeed observed the species changes after inoculating the high-saline cell assemblies into f/2-enriched low-saline field water for another three weeks—just left the unknown pennates as dominating species (data not shown). It is consistent with the results of Hernando et al. (2015) who reported the big centric diatoms are replaced by small pennate ones after 8 d exposure to low salinity in a coastal area of Antarctica. In this study, we used solely larger cells (>20 μm) that took up ~40% of total field cell assemblies (Huang et al., 2012). For small cells however, they have high surface to volume ratios and are more vulnerable to environmental changes than large ones, no exception to the salt stress (Raven, 1998; Finkel et al., 2010). So, rapid recovery of phytoplankton from the acute osmotic stress would be tempered if considering the whole cell assemblies.

Phytoplankton assemblies from the Jiulong River Estuary proved strongly capable to recover from osmotic stress (Figs 2–5), which, together with a wide salinity range (Table 1), points to the mechanisms regulating intracellular salt pressure. Up to now, it still remains unclear that the mechanisms of the acute salt stress effects on photosynthetic performances of phytoplankton assemblies. In particular the metabolic processes in a certain algal species under the changed salinity are not known, although the release of low molecular weight compounds of e.g. amino acids and glucoses to environments has been proposed to be one of the main mechanisms of response to osmotic stress in diatoms (Rijstenbil et al., 1989a, b). Some authors considered that the osmotic stress mainly contribute adverse effects to the growth of phytoplankton (Lu and Zhang, 1999; Licursi et al., 2006; D'ors et al., 2016); while others suggested that abundant nutrients interact with high salt tolerance to make them to bloom frequently in estuaries although the salinity varies drastically (Lim and Ogata, 2005; Doucette et al., 2008). However, our results indicate that estuarine phytoplankton could rapidly recover from the osmotic stress; it to some extent reconcile the phenomenon that phytoplankton are abundant in estuaries in spite of the rough salinity environments.

Acknowledgements

We are grateful to the experimental helps of Ying Zheng, Wei Li and Guiyuan Yang and nutrient analysis of Yongming Huang.

References

Allakhverdiev S I, Nishiyama Y, Miyairi S, et al. 2002. Salt stress inhibits the repair of photodamaged photosystem II by suppressing the transcription and translation of *psbA* genes in *Synechocystis*. Plant Physiology, 130(3): 1443–1453, doi: 10.1104/pp.011114

Armstrong F A J, Stearns C R, Strickland J D H. 1967. The measurement of upwelling and subsequent biological process by means of the Technicon Autoanalyzer? and associated equipment. Deep Sea Research and Oceanographic Abstracts, 14(3): 381–389, doi: 10.1016/0011-7471(67)90082-4

Brand L E. 1984. The salinity tolerance of forty-six marine phytoplankton isolates. Estuarine, Coastal and Shelf Science, 18(5): 543–556, doi: 10.1016/0272-7714(84)90089-1

Cai Aizhi, Cai Yuee, Zhu Xiaoning, et al. 1991. Diffusion and modern sedimentation of seaward-transporting discharges in the estuary of Jiulongjiang River, Fujian Province. Marine Geology & Quaternary Geology (in Chinese), 11(1): 57–67

Cao Zhenrui, Huang Bangqin, Liu Yuan, et al. 2005. Distribution characteristics of size-fractionated chlorophyll a in Xiamen waters. Journal of Oceanography in Taiwan Strait (in Chinese), 24(4): 493–501

Cao Wenzhi, Huang Zheng, Zhai Weidong, et al. 2015. Isotopic evidence on multiple sources of nitrogen in the northern Jiulong River, Southeast China. Estuarine, Coastal and Shelf Science, 163: 37–43, doi: 10.1016/j.ecss.2015.05.042

Chen Baohong, Chen Changping, Chen Jinmin, et al. 2012. Variations of nutrient content and ratios and their impact on phytoplankton community in Xiamen waters. Journal of Oceanography in Taiwan Strait (in Chinese), 31(2): 246–253

Chen Baohong, Ji Weidong, Chen Jinmin, et al. 2013a. Characteristics of nutrients in the Jiulong River and its impact on Xiamen Water, China. Chinese Journal of Oceanology and Limnology, 31(5): 1055–1063, doi: 10.1007/s00343-013-2263-3

Chen Nengwang, Peng Benrong, Hong Huasheng, et al. 2013b. Nutrient enrichment and N:P ratio decline in a coastal bay-river system in southeast China: The need for a dual nutrient (N and P) management strategy. Ocean & Coastal Management, 81: 7–13

Cloern J E. 1999. The relative importance of light and nutrient limitation of phytoplankton growth: a simple index of coastal ecosystem sensitivity to nutrient enrichment. Aquatic Ecology, 33(1): 3–15, doi: 10.1023/A:1009952125558

Domingues R B, Anselmo T P, Barbosa A B, et al. 2010. Tidal variabil-

ity of phytoplankton and environmental drivers in the freshwater reaches of the Guadiana Estuary (SW Iberia). International Review of Hydrobiology, 95(4–5): 352–369, doi: 10.1002/iroh.v95:4/5

D'ors A, Bartolomé M C, Sánchez-Fortún S. 2016. Repercussions of salinity changes and osmotic stress in marine phytoplankton species. Estuarine, Coastal and Shelf Science, 175: 169–175, doi: 10.1016/j.ecss.2016.04.004

Doucette G J, King K L, Thessen A E, et al. 2008. The effect of salinity on domoic acid production by the diatom Pseudo-Nitzschia multiseries. Nova Hedwigia Beiheft, 133: 31–46

Finkel Z V, Beardall J, Flynn K J, et al. 2010. Phytoplankton in a changing world: cell size and elemental stoichiometry. Journal of Plankton Research, 32(1): 119–137, doi: 10.1093/plankt/fbp098

Gao Guang, Xia Jianrong, Yu Jinlan, et al. 2018. Physiological response of a red tide alga (*Skeletonema costatum*) to nitrate enrichment, with special reference to inorganic carbon acquisition. Marine Environmental Research, 133: 15–23, doi: 10.1016/j.marenvres.2017.11.003

Genty B, Briantais J M, Baker N R. 1989. The relationship between the quantum yield of photosynthetic electron transport and quenching of chlorophyll fluorescence. Biochimica et Biophysica Acta (BBA)-General Subjects, 990(1): 87–92, doi: 10.1016/S0304-4165(89)80016-9

Giacobbe M G, Oliva F D, Maimone G. 1996. Environmental factors and seasonal occurrence of the dinoflagellate *Alexandrium minutum*, a PSP potential producer, in a Mediterranean lagoon. Estuarine, Coastal and Shelf Science, 42(5): 539–549, doi: 10.1006/ecss.1996.0035

Häubner N, Sylvander P, Vuori K, et al. 2014. Abiotic stress modifies the synthesis of alpha-tocopherol and beta-carotene in phytoplankton species. Journal of Phycology, 50(4): 753–759, doi: 10.1111/jpy.2014.50.issue-4

Hernando M, Schloss I R, Malanga G, et al. 2015. Effects of salinity changes on coastal Antarctic phytoplankton physiology and assemblage composition. Journal of Experimental Marine Biology and Ecology, 466: 110–119, doi: 10.1016/j.jembe.2015.02.012

Holm-Hansen O, Helbling E W. 1995. Técnicas para la medición de la productividad primaria en el fitoplancton. In: Alveal K, Ferrario M E, Oliveira E C, et al, eds. Manual de Métodos Ficológicos. Concepción: Universidad de Concepción, 329–350

Huang Xuguang, Guo Donghui, Xiao Wupeng, et al. 2012. The relationship between quantitative changes of microplankton and population dynamics of small medusa in the Jiulong River estuary in spring of 2011. Oceanologia et Limnologia Sinica (in Chinese), 43(3): 579–583

Huang Liangmin, Jian Weijun, Song Xingyu, et al. 2004. Species diversity and distribution for phytoplankton of the Pearl River estuary during rainy and dry seasons. Marine Pollution Bulletin, 49(7–8): 588–596, doi: 10.1016/j.marpolbul.2004.03.015

Li Ying, Cao Wenzhi, Su Caixia, et al. 2011a. Nutrient sources and composition of recent algal blooms and eutrophication in the northern Jiulong River, Southeast China. Marine Pollution Bulletin, 63(5–12): 249–254, doi: 10.1016/j.marpolbul.2011.02.021

Li Gang, Gao Kunshan, Yuan Dongxing, et al. 2011b. Relationship of photosynthetic carbon fixation with environmental changes in the Jiulong River estuary of the South China Sea, with special reference to the effects of solar UV radiation. Marine Pollution Bulletin, 62(8): 1852–1858, doi: 10.1016/j.marpolbul.2011.02.050

Li Gang, Lin Qiang, Lin Junda, et al. 2014. Environmental gradients regulate the spatial variations of phytoplankton biomass and community structure in surface water of the Pearl River estuary. Acta Ecologica Sinica, 34(2): 129–133, doi: 10.1016/j.chnaes.2014.01.002

Licursi M, Sierra M V, Gómez N. 2006. Diatom assemblages from a turbid coastal plain estuary: Río de la Plata (South America). Journal of Marine Systems, 62(1–2): 35–45, doi: 10.1016/j.jmarsys.2006.03.002

Lim P T, Ogata T. 2005. Salinity effect on growth and toxin production of four tropical *Alexandrium* species (Dinophyceae). Toxicon, 45(6): 699–710, doi: 10.1016/j.toxicon.2005.01.007

Liu Guangping, Hu Jianyu, Chen Zhaozhang, et al. 2008. Distribution characteristics of sea surface salinity and its relations to tide in Jiulongjiang estuary-Xiamen Bay. Journal of Xiamen University (Natural Science) (in Chinese), 47(5): 710–713

Liu Lemian, Yang Jun, Yu Xiaoqing, et al. 2013. Patterns in the composition of microbial communities from a subtropical river: effects of environmental, spatial and temporal factors. PLoS One, 8(11): e81232, doi: 10.1371/journal.pone.0081232

Lu Chongming, Zhang Jianhua. 1999. Effects of salt stress on PSII function and photoinhibition in the cyanobacterium *Spirulina platensis*. Journal of Plant Physiology, 155(6): 740–745, doi: 10.1016/S0176-1617(99)80091-1

Mo Yu, Lin Lizhen, Zheng Liping, et al. 2013. Phytoplankton phosphorus stress of Jiulongjiang River-Estuary and adjacent waters system in summer. Oceanologia et Limnologia Sinica (in Chinese), 44(1): 241–248

Murphy J, Riley J P. 1962. A modified single solution method for the determination of phosphate in natural waters. Analytica Chimica Acta, 27: 31–36, doi: 10.1016/S0003-2670(00)88444-5

Muylaert K, Sabbe K, Vyverman W. 2009. Changes in phytoplankton diversity and community composition along the salinity gradient of the Schelde estuary (Belgium/The Netherlands). Estuarine, Coastal and Shelf Science, 82(2): 335–340, doi: 10.1016/j.ecss.2009.01.024

Nche-Fambo F A, Scharler U M, Tirok K. 2015. Resilience of estuarine phytoplankton and their temporal variability along salinity gradients during drought and hypersalinity. Estuarine, Coastal and Shelf Science, 158: 40–52, doi: 10.1016/j.ecss.2015.03.011

Pai Sucheng, Tsau Y J, Yang T I. 2001. pH and buffering capacity problems involved in the determination of ammonia in saline water using the indophenol blue spectrophotometric method. Analytica Chimica Acta, 434(2): 209–216, doi: 10.1016/S0003-2670(01)00851-0

Porra R J. 2002. The chequered history of the development and use of simultaneous equations for the accurate determination of chlorophylls a and b. Photosynthesis Research, 73(1–3): 149–156

Radchenko I G, Il'iash L V. 2006. Growth and photosynthetic activity of diatom *Thalassiosira weissflogii* at decreasing salinity. Izvestiia Akademii Nauk. Seriia Biologicheskaia, (3): 306–313

Raven J A. 1998. The twelfth tansley lecture, small is beautiful: the picophytoplankton. Functional Ecology, 12(4): 503–513, doi: 10.1046/j.1365-2435.1998.00233.x

Rijstenbil J W, Mur L R, Wijnholds J J, et al. 1989a. Impact of a temporal salinity decrease on growth and nitrogen metabolism of the marine diatom *Skeletonema costatum* in continuous cultures. Marine Biology, 101(1): 121–129, doi: 10.1007/BF00393485

Rijstenbil J W, Wijnholds J A, Sinke J J. 1989b. Implications of salinity fluctuation for growth and nitrogen metabolism of the marine diatom *Ditylum brightwellii* in comparison with *Skeletonema costatum*. Marine Biology, 101(1): 131–141, doi: 10.1007/BF00393486

Tang Rongkun, He Qing, Ji Weidong, et al. 2010. Characteristics of temporal and spatial variations in chlorophyll contents of waters around Xiamen Island in 2005~2007. Journal of Oceanography in Taiwan Strait (in Chinese), 29(3): 342–351

Thessen A E, Dortch Q, Parsons M L, et al. 2005. Effect of salinity on *Pseudo-Nitzschia* species (Bacillariophyceae) growth and distribution. Journal of Phycology, 41(1): 21–49, doi: 10.1111/jpy.2005.41.issue-1

Tian Yongqiang, Huang Bangqin, Yu Chaochao, et al. 2014. Dynamics of phytoplankton communities in the Jiangdong Reservoir of Jiulong River, Fujian, South China. Chinese Journal of Oceanology and Limnology, 32(2): 255–265, doi: 10.1007/s00343-014-3158-7

Van Kooten O, Snel J F H. 1990. The use of chlorophyll fluorescence nomenclature in plant stress physiology. Photosynthesis Research, 25(3): 147–150, doi: 10.1007/BF00033156

Villafañe V, Reid F. 1995. Métodos de microscopía para la cuantificación del fitoplancton. In: Alveal K, Ferrario M E, Oliveira E C, et al., eds. Manual de Métodos Ficológicos. Concepción: Universidad de Concepción, 169–185

Wang Jia, Hong Huasheng, Zhou Lumin, et al. 2013. Numerical modeling of hydrodynamic changes due to coastal reclamation projects in Xiamen Bay, China. Chinese Journal of Oceanology and Limnology, 31(2): 334–344, doi: 10.1007/s00343-013-2109-z

Wang Weiqiang, Huang Shanggao, Gu Deyu, et al. 1986. Mixing characters of fresh water with sea water in the Jiulong Jiang estuary, Fujian. Journal of Oceanography in Taiwan Strait (in Chinese), 5(1): 10–17

Wang Yongming, Liu Lemian, Chen Huihuang, et al. 2015b. Spatiotemporal dynamics and determinants of planktonic bacterial and microeukaryotic communities in a Chinese subtropical river. Applied Microbiology and Biotechnology, 99(21): 9255–9266, doi: 10.1007/s00253-015-6773-0

Wang Guizhi, Wang Zhangyong, Zhai Weidong, et al. 2015a. Net subterranean estuarine export fluxes of dissolved inorganic C, N, P, Si, and total alkalinity into the Jiulong River estuary, China. Geochimica et Cosmochimica Acta, 149: 103–114, doi: 10.1016/j.gca.2014.11.001

Wood E D, Armstrong F A J, Richards F A. 1967. Determination of nitrate in sea water by cadmium-copper reduction to nitrite. Journal of the Marine Biological Association of the United Kingdom, 47(1): 23–31, doi: 10.1017/S002531540003352X

Wu Gaojie, Cao Wenzhi, Huang Zheng, et al. 2017. Decadal changes in nutrient fluxes and environmental effects in the Jiulong River Estuary. Marine Pollution Bulletin, 124(2): 871–877, doi: 10.1016/j.marpolbul.2017.01.071

Yan Xiuli, Zhai Weidong, Hong Huasheng, et al. 2012. Distribution, fluxes and decadal changes of nutrients in the Jiulong River Estuary, Southwest Taiwan Strait. Chinese Science Bulletin, 57(18): 2307–2318, doi: 10.1007/s11434-012-5084-4

Yi Rong, Tan Yehui, Wang Shengfu, et al. 2014. Cell size dependent responses of phytoplankton assemblages to nitrate and phosphate additions in surface waters of the northern South China Sea. Open Journal of Marine Science, 4(2): 44564

Yin Kedong, Qian Peiyuan, Wu M C S, et al. 2001. Shift from P to N limitation of phytoplankton growth across the Pearl River estuarine plume during summer. Marine Ecology Progress Series, 221: 17–28, doi: 10.3354/meps221017

Zhang Shuting, Lv Lu, Zhang Yongli, et al. 2013. Occurrence and variations of five classes of antibiotic resistance genes along the Jiulong River in southeast China. Journal of Environmental Biology, 34: 345–351